



THREE-DIMENSIONAL GROUND MOTION SCALING FOR HIGHWAY BRIDGES

K.R. Mackie¹ and B. Stojadinovic²

ABSTRACT

Recent enhancements to and adoption of nonlinear time history finite element analysis for seismic response assessment of structures have motivated the need for suites of ground motions that represent expected seismicity at all hazard levels of interest. The availability of high intensity records often necessitates the need for scaling of ground motions. This approach is intrinsic to use of such procedures as incremental dynamic analysis. Recent research has produced recommendations for selection and scaling of ground motions for use in such analyses based on magnitude, distance, and epsilon. However, research has largely been limited to two-dimensional planar analysis of buildings. Three-dimensional finite element models with three or more components of ground motion input and the corresponding three-dimensional response of structures can differ considerably from such two-dimensional analyses. This paper considers a typical California reinforced concrete highway overpass bridge in the three-dimensional scaling of records for use in incremental dynamic analysis. Such bridges exhibit distinct transverse and longitudinal response shapes for the first two modes. Comparisons are made between scaling the motions to the spectral ordinate at the fundamental period of the structure, an average of the longitudinal and transverse periods, a square-root-sum-of-squares combination, an average of spectral quantities over a period band, and different scale factors for the longitudinal and transverse components based on their respective spectral ordinate. Scaled results are then compared with cloud analysis of un-scaled records using a larger catalog of ground motions. Recommendations for three-dimensional scaling of ground motions for bridge structures are presented.

Introduction

Considerable attention has been devoted to the two-dimensional idealization, modeling, excitation, and response of structures under large earthquake demands. In particular, seismic demands are quantified using nonlinear time history analysis for a particular structural model and a selection of ground motion records. Many recent examples of analytical studies of this nature are available in the literature, especially those studies applied to buildings (e.g., Liu and Goel, 2006; Liao and Wen, 2004; Haselton and Baker, 2006; Kunnath and Kalkan, 2005). Fewer examples exist for bridges (e.g., Shantz, 2006). However, a common theme amongst all of the studies is the need for adequate selection and scaling of the ground motion records used to represent the hazard environment expected for the structure. This is particularly relevant when existing recorded motions do not exist (as is the case for the central US) or when extreme high-intensity records are needed for collapse simulation.

¹Assistant Professor, Dept. of Civil and Env. Engineering, University of Central Florida, Orlando, FL 32816-2450

²Associate Professor, Dept. of Civil and Env. Engineering, University of California, Berkeley, CA 94720-1710

When considering the two-dimensional analysis of structures, numerous guidelines have been established for the selection of ground motion records (Iervolino and Cornell, 2005) based on properties of the earthquake such as magnitude and properties of the site such as closest distance to fault and soil type. Additional studies have suggested the selection of ground motion records taking into account the spectral shape as well (Baker and Cornell, 2005; Bray et al 2002; Haselton and Baker 2006). The measure of spectral shape used in these studies is epsilon, or the number of standard deviations the response spectral ordinate falls from a predicted median spectral value. Spectral shape information is also included in scale factors derived from the inelastic SDOF surface of Shantz (2006). The optimal scale factor (Shantz, 2006) is similar to epsilon as both show the deviation of a particular record from a common design value, such as that obtained from an attenuation relationship. Complementary efforts, such as those of the ATC-58 project (<http://www.atcouncil.org/atc-58.shtml>) and next generation attenuation models (<http://peer.berkeley.edu/lifelines/repngamodels.html>), have contributed to the guidelines for selection of and the availability of records for use. However, as mentioned, the studies have been primarily 2D or uniform scaling of all three-dimensional components. Scaling of records is usually accomplished by the amplitude scaling of records to a common intensity measure or spectral value, such as the first-mode spectral acceleration. Scaling several records to a single intensity is termed a stripe analysis, whereas completing a sweep through a larger IM range by scaling several records is termed incremental dynamic analysis (IDA).

Incremental dynamic analysis (e.g., Vamvatsikos and Cornell, 2002) is used as the method of probabilistic seismic demand analysis in this paper. IDA was previously applied to the three-dimensional analysis of steel frame buildings (Vamvatsikos, 2006). However, the focus of the study was on marginal demand models in each orthogonal building direction and reducing the uncertainty in predicting these demands through the use of a vector of intensities. This study does not attempt to reduce the dispersion of demand models from three-dimensional analysis by considering a vector of IMs. Rather, this study is focused on an optimal method for scaling records in three dimensions to reproduce the demand models obtained from a larger catalog of non-scaled records. Possible byproducts of scaling in three dimensions are bias in the expected values, disparate scale factors in the orthogonal non-scaling directions, and accounting for spectral shape at more than one structural period. A typical bridge structure is selected for the investigation of the three-dimensional scaling of ground motion records for IDA usage in this paper. It is demonstrated that careful selection of records based on spectral shape information at the fundamental period in each bridge direction, or the independent scaling of records in each direction lead to the best agreement with un-scaled records.

Bridge Model

The Federal Highway Administration (FHWA) maintains a national bridge inventory (<http://www.fhwa.dot.gov/bridge/nbi.htm>). Highway bridges are classified according to material type and structure type. From the 2003 census of California bridges, 15670 (66%) bridges were constructed of either concrete or pre-stressed concrete. The structural types included slab, stringer/multi-beam or girder, box beam or girder, and culvert. A total of 10291 (43%) of the total are either box beam or girder or culvert type. Additionally, from highway network studies specifically on the San Francisco Bay Area (Kiremidjian 2006), a total of 2640 bridges were further characterized by type, year built, number of spans, etc. Of this subset, 1415 (54%) were reinforced concrete box beam, girder, or culvert, and 763 (29%) were single-column bent box girder bridges alone. Descriptions of the individual bridges used, typical of new designs in California, and their finite element model representations are described in previous studies on California highway bridges (Mackie and Stojadinovic 2005). These bridges were described in terms of structural design parameters (such as column height, longitudinal reinforcing ratio, soil properties, etc). For this study, a single bridge configuration is selected from this previous study. The highway overpass bridge has two equal continuous box-girder spans ($L = 27.4\text{m}$), a single bent ($H_t = 9.1\text{m}$) with a single column ($D_c = 1.14\text{m}$) continuing into an integral pile shaft foundation, simulated soil response through nonlinear p - y springs located along the pile shaft length, and a simplified abutment model with longitudinal (10cm gap) and transverse components. The column has 2% longitudinal steel and 1% transverse steel reinforcement ratios. The bridge is assumed to be on a cohesionless sand site with uniform soil profile

properties. The water table was assumed to be below the base of the pile shafts.

The bridge was designed according to Caltrans' Seismic Design Criteria (Caltrans 2004) for reinforced concrete bridges. Consistent with the displacement-based design approach used by Caltrans for new bridges, it was assumed that reinforced concrete columns developed plastic hinges in flexure rather than experienced shear failure. The bridge deck was designed as a typical Caltrans reinforced concrete box girder section for a three-lane roadway. The nonlinear engine selected for modeling was the PEER OpenSees (<http://opensees.berkeley.edu>) platform. Bridge columns, pile shafts, and deck elements are modeled using three-dimensional elements with fiber cross-sections, including shear deformations. The circular column cross-sections have perimeter longitudinal reinforcing bars and spiral confinement. Several modeling improvements were made above and beyond those listed in Mackie and Stojadinovic (2005). Specifically, softening in the steel constitutive model is no longer accomplished by a linear softening backbone curve. Rather, a material that takes into account low-cycle fatigue using a rudimentary rainflow counting method is incorporated (Uriz 2005). The properties of the constitutive model were customized for reinforcing bars based on experimental low-cycle fatigue tests by Brown and Kunnath (2004).

An abutment model was also incorporated in the bridge longitudinal and transverse directions. This model is a simple derivative of the more complex spring model used in Mackie and Stojadinovic (2006). The longitudinal direction has a stiffness derived from the series response of bearing pads between the deck and stemwall and the longitudinal response of the backwall/fill/pile system. The elastomeric bearing pads underneath each of the box girder webs are modeled explicitly by the introduction of an array of elements in the bridge transverse direction that physically account for the width of the box. The bearing pad elements are interfaced with another transverse array of elements using spring constants derived from Caltrans SDC recommendations for longitudinal response derived from large-scale experimental tests. The transverse direction was simplified in this study to include the same bearing pads acting in series with a stiffness of the backfill/pile system modified by wing wall participation factors. Details of the abutment model are provided in Mackie and Stojadinovic (2006). The shear key model is not included in this study.

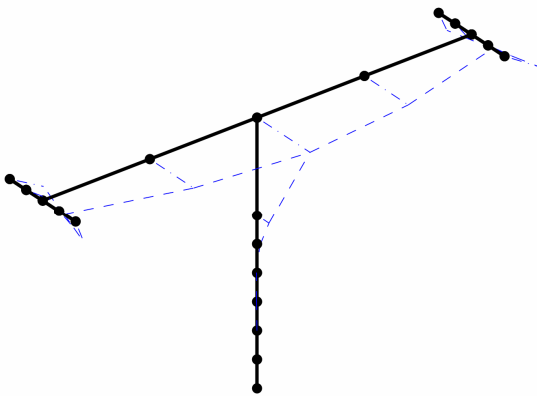


Figure 1. Mode shape of fundamental transverse period ($T_1=1.19$ sec).

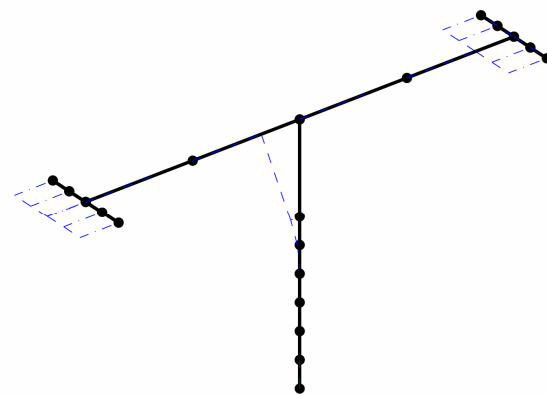


Figure 2. Mode shape of fundamental longitudinal period ($T_2=0.91$ sec).

The longitudinal response of the abutment is not mobilized until gap closure; however, the transverse direction is initially restrained. Nevertheless, the transverse direction is more flexible in this model, as indicated by the first two mode shapes of the bridge. The fundamental transverse ($T_1 = 1.19$ sec) mode shape is shown in Figure 1, and the fundamental longitudinal ($T_2 = 0.91$ sec) mode shape is shown in Figure 2. The separation of primary modal response in each of the bridge directions makes it possible to scrutinize ground motion scaling independently in each direction. The six nodes at the base of the column are below grade.

Probabilistic Seismic Demand Analysis

Nonlinear dynamic time history analysis was performed on the bridge using bins of recorded ground motion acceleration time histories. Two orthogonal lateral components and a single vertical component of each recorded ground motion were applied simultaneously to the three-dimensional bridge model. Probabilistic seismic demand analysis (PSDA) was performed using both the cloud and incremental dynamic techniques. PSDA and details of each method are outlined in more detail in Mackie and Stojadinovic (2005). In summary, the cloud method applies a larger catalog of unscaled ground motion records collected into magnitude-distance bins to the bridge. Incremental dynamic analysis describes a general technique for scaling of ground motions to common earthquake intensities (Vamvatsikos 2002). For each analysis performed, the maximum response quantity of interest is retained. A statistical relationship between these peak response quantities and a measure descriptive of the ground motion intensity is sought. The PEER center designates the response measures as engineering demand parameters (EDPs) and earthquake intensity descriptors as intensity measures (IMs). The relationship between IM and EDP is denoted a probabilistic seismic demand model (PSDM).

The IM used in this paper is the spectral acceleration of a 5% viscously damped single-degree-of-freedom system at a specified period. $Sa(T_T)$ is defined as the spectral acceleration at the fundamental transverse period (T_T) computed for the ground motion component in the bridge transverse direction. $Sa(L_L)$ is the spectral acceleration at the fundamental longitudinal period (T_L) in the longitudinal direction. The only EDP considered in this paper is the maximum tangential drift ratio (Δ) of the column. The tangential drift ratio is defined as the larger of the column displacements above and below the column inflection point, normalized by the respective distances of the locations of maximum displacement to the inflection point. The location of the inflection point moves during transient analysis; therefore, it is necessary to calculate the drift ratio at each time step. The baseline results used in this paper against which all ground motion scaling results are compared is based on the cloud analysis method. The same seven ground motion bins used in Mackie and Stojadinovic (2006) are used in this study.

Ten different ground motion scaling strategies were employed for comparison to the cloud analysis results. The scale factor applied to the bridge transverse and longitudinal directions are listed in Table 1. Also listed in the table are the parameters describing the marginal best fit relationship in each bridge direction. The best fit (median) is assumed to be of a power-law form, have constant log dispersion, s , and the distribution of EDP conditioned on IM is lognormal. The method designated as IDA 1 is the traditional IDA approach of scaling all components of a record to $Sa(T_T)$. In this case, the primary mode of response for the first mode is transverse; therefore, the single value of $Sa(T_T)$ is used for scaling. The scaling methods designated as IDA 2, 3, and 6 are examples of spectral combinations, and IDA 5 is an example of scaling to a vector of IMs. The evolution of the different scaling strategies is evident when plotting families of intensities in the $Sa(T_T)$ - $Sa(T_L)$ plane, as shown in Figure 3. The traditional transverse (IDA 1) and longitudinal (IDA 8) scaling strategies are shown in the upper-right pane of the figure. The spectral combinations are compared in the lower two panes of the figure. For the IDA 5 case, all EDP realizations fall on the vertical line through each point in the upper-left pane. The data points from cloud analysis are also included for comparison. It should be noted that the range of intensities considered for the IDA analyses were intentionally selected to coincide with that from cloud analysis. It was not an intention of this study to include the effects of collapse.

A pitfall unique to the three-dimensional seismic analysis of structures is scaling the orthogonal component disproportionately even when considering epsilon for the direction under consideration. The concept is illustrated for the FAR (Northridge) record in Figure 4. The top pane shows the transverse response spectrum as compared to the Abrahamson and Silva attenuation relationship (Abrahamson and Silva, 1997). The transverse component is a negative epsilon record and is scaled up to reach the median spectrum from the attenuation relationship. However, the orthogonal component (longitudinal direction) is a positive epsilon record that reaches spectral accelerations close to 1.5 g when scaled by the same amount as the transverse record. The relationship between epsilon values is therefore an important quantity and is listed for the randomly selected IDA records along with the epsilon value in each direction

in Table 2. Another issue pertaining to nonlinear dynamic time history analysis (not unique to 3D) is numerical instability exhibited by structures subjected to records with large scale factors. This is an issue not necessarily addressed by the ϵ_L/ϵ_T ratio. Therefore, scale factors are also listed in Table 2. These scale factors are maxima and minima over all the scaling strategies; therefore, individual records can be evaluated. For example, the A-KOD record (Livermore earthquake) has large scale factors and is in part the cause of numerous numerical convergence or instability issues. Individual time history results with numerical instabilities were removed when generating PSDMs.

Table 1. Summary of analysis method scale factors and resulting spectral acceleration versus tangential drift ratio PSDM marginal distribution parameters ($\ln(\Delta) = A + B \ln(IM) + \sigma \epsilon$).

Method	Transverse scale factor	Longitudinal scale factor	Transverse marginal (A, B, σ)	Longitudinal marginal (A, B, σ)
Cloud	2	2	-6.05, 1.04, 0.19	-5.69, 0.88, 0.16
IDA – 1	$Sa(T_T)$	$Sa(T_T)$	-6.79, 1.16, 0.24	-6.58, 1.02, 0.22
IDA – 2	$(Sa(T_T) + Sa(L_L))/2$	$(Sa(T_T) + Sa(L_L))/2$	-6.66, 1.14, 0.21	-6.08, 0.93, 0.16
IDA – 3	$\sqrt{Sa(T_T)^2 + Sa(L_L)^2}$	$\sqrt{Sa(T_T)^2 + Sa(L_L)^2}$	-6.45, 1.10, 0.16	-5.96, 0.91, 0.13
IDA – 4	$Sa(T_T)$	$Sa(T_T)$	-6.73, 1.15, 0.24	-6.56, 1.01, 0.23
IDA – 5	$Sa(T_T)$	$Sa(L_L)$	-6.60, 1.12, 0.24	-6.07, 0.93, 0.12
IDA – 6	$\sqrt{Sa(T_T)Sa(L_L)}$	$\sqrt{Sa(T_T)Sa(L_L)}$	-6.73, 1.15, 0.23	-6.15, 0.94, 0.16
IDA – 7	$Sa(L_L)$	$Sa(L_L)$	-6.81, 1.17, 0.26	-6.25, 0.95, 0.15
IDA – 8	$Sa(L_L)$	$Sa(L_L)$	-6.67, 1.14, 0.21	-6.05, 0.92, 0.13
IDA – 9	$Sa(T_L)$	$Sa(T_L)$	-6.81, 1.17, 0.24	-6.17, 0.91, 0.17
IDA – 10	$Sa(L_L)$	$Sa(L_L)$	-6.69, 1.15, 0.22	-5.98, 0.91, 0.15

Table 2. Ground motions used for (randomly chosen record) IDA analysis (IDA = 1 to 10), including epsilon values and scale factors in each direction.

Bin	Motion	$\epsilon(L_L)$	$\epsilon(T_T)$	$\epsilon(L_L)/\epsilon(T_T)$	SF _{min}	SF _{max}
kLMSR	HCH	1.686	0.974	1.731	1.5	4.3
	LOS	0.89	-0.208	-4.279	1.5	6.1
kLMLR	A-ELC	-0.011	1.108	-0.010	5.2	10.5
	SLC	1.173	1.428	0.821	2.4	4.1
kSMSR	A-KOD	0.279	1.371	0.204	6.3	18.3
	H-CHI	1.533	0.799	1.919	1.9	6.5
kSMLR	H-DLT	2.224	1.02	2.180	2.0	7.7
	M-CAP	0.021	-0.265	-0.079	6.2	26.1
I880_ida_1	Cclyd	-0.364	-1.083	0.336	5.4	19.9
	Andd	-0.985	-0.415	2.373	4.3	9.2
I880_ida_5	Gav	-1.34	-1.29	1.039	4.5	8.1
	Gil6	0.887	-0.185	-4.795	1.5	6.8
I880_ida_9	Srtg	-0.109	-0.399	0.273	1.9	4.6
	Temb	-0.999	-1.401	0.713	5.8	15.9

Table 3. Ground motions used for (epsilon-selected record) IDA analysis (IDA = 101 to 110), including epsilon values and scale factors in each direction.

Bin	Motion	$\epsilon(L)$	$\epsilon(T)$	$\epsilon(L)/\epsilon(T)$	SF _{min}	SF _{max}
eLMSR	G04	0.177	0.083	2.133	2.1	3.5
	HDA	1.654	0.998	1.657	1.3	3.6
eLMLR	A2E	0.581	1.254	0.463	3.3	6.0
	SLC	1.173	1.43	0.821	1.8	4.1
eSMSR	A-DWN	0.495	0.88	0.563	2.9	9.0
	H-CHI	1.533	0.799	1.919	1.9	4.4
eSMLR	H-DLT	2.224	1.02	2.18	1.8	5.3
	M-HCH	0.877	0.837	1.048	4.3	8.1
el880	Clyd	0.761	0.331	2.299	0.8	2.1
	Srtg	-0.109	-0.399	0.273	1.6	3.2
eVN_1	Env1	0.667	0.751	0.888	1.2	2.9
	Vnuy	0.534	0.574	0.93	1.4	2.2
eVN_2	Whox	0.701	0.874	0.802	1.9	3.3
	Glen	1.898	1.514	1.254	1.3	3.0

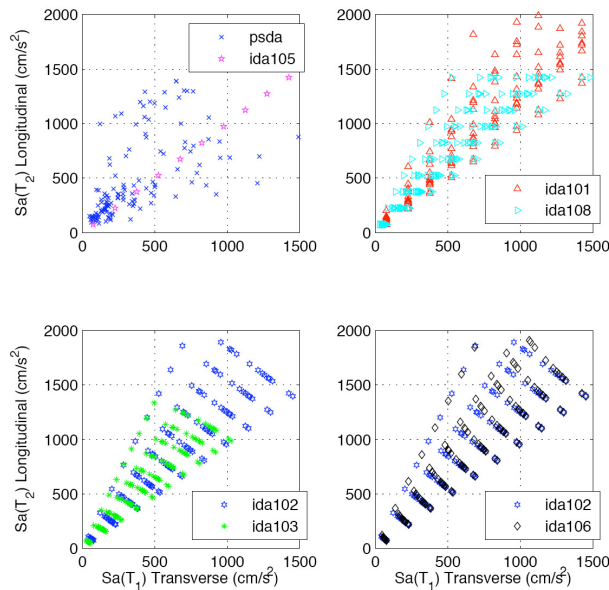


Figure 3. Evolution of IDA scaling options looking at both transverse and longitudinal intensities.

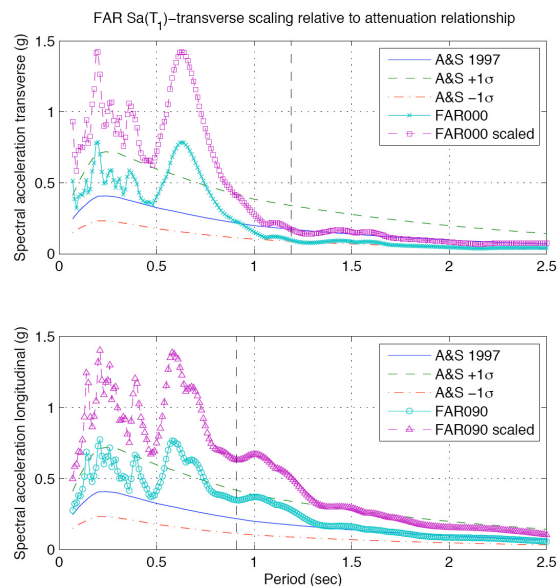


Figure 4. Longitudinal and transverse response spectra comparison of a negative ϵ_L/ϵ_T record (FAR - Northridge).

Results

Standard PSDMs are plotted for several of the ground motion scaling strategies. Marginal PSDMs for the traditional scaling approach (IDA 1) are shown in Figure 5 for the transverse bridge direction and Figure 6 for the longitudinal direction. As is evident in both the scaling direction (transverse) and orthogonal direction (longitudinal), the IDA = 1 median is conservatively biased. This is a result observed by others when considering records chosen at random for the IDA analysis (Baker and Cornell, 2005; Haselton and Baker, 2006). The bias is larger in the orthogonal component than in the scaling direction as no attention was given to the resulting scale factors in the longitudinal direction. For comparison, a more refined selection of records was made to determine if the bias was attributable to the selection of records by epsilon. The resulting motions chosen, epsilon values, and the ratio of epsilon values are shown in

Table 3. The refined selection of records are designated as 101 for scaling type 1, 102 for scaling type 2, etc. As evidenced from the epsilon ratio, it is a good individual value for the selection of records. A negative sign implies the longitudinal and transverse components fall on opposite sides of the attenuation median and therefore, scale factors may be problematic. Extremely large (> 10) or small (< 0.1) values indicate that the longitudinal and transverse motions are dominant, respectively. A magnitude close to 1 and a positive sign is therefore a desirable target to minimize issues when scaling orthogonal records.

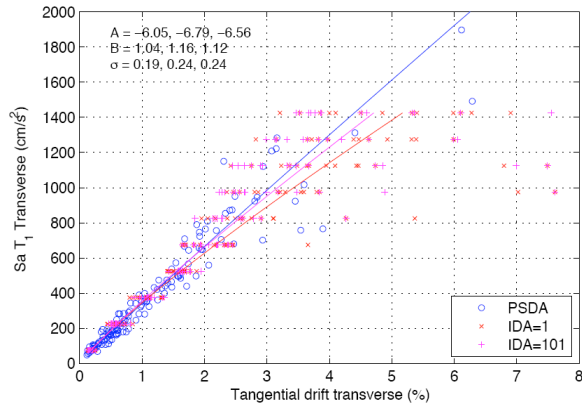


Figure 5. PSDM showing $Sa(T_1)$ - Δ marginal in the transverse direction for IDA scaling option 1.

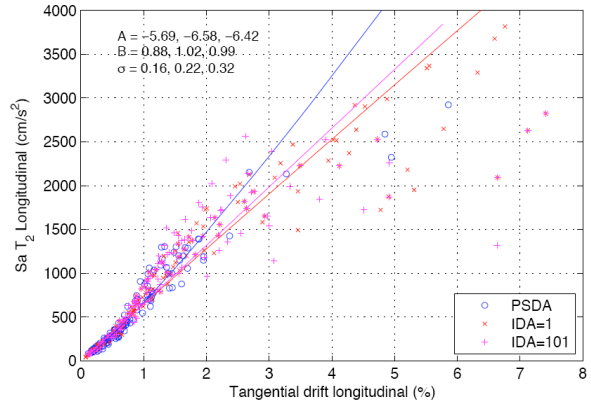


Figure 6. PSDM showing $Sa(T_2)$ - Δ marginal in the longitudinal direction for IDA scaling option 1.

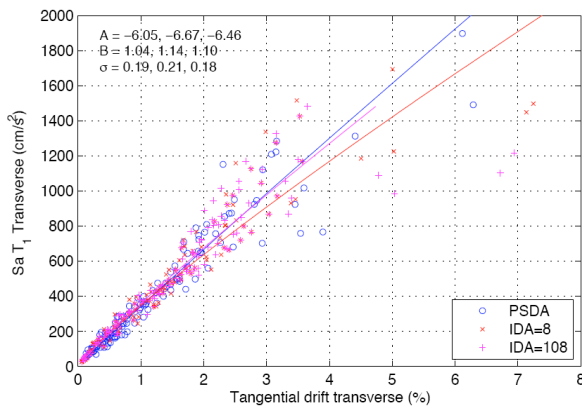


Figure 7. PSDM showing $Sa(T_1)$ - Δ marginal in the transverse direction for IDA scaling option 8.

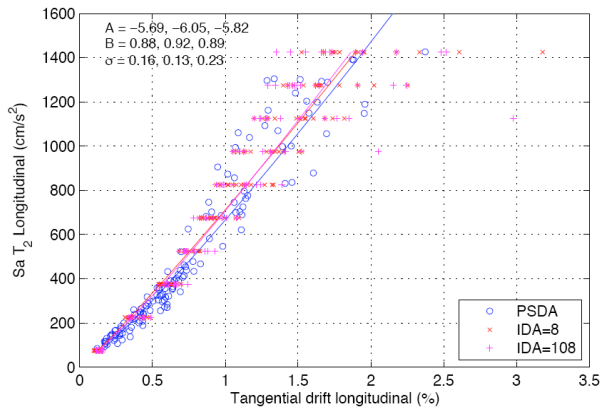


Figure 8. PSDM showing $Sa(T_2)$ - Δ marginal in the longitudinal direction for IDA scaling option 8.

Both the original set (IDA 1) and the refined set (IDA 101) of records are plotted in the marginal PSDMs shown in Figure 5 (transverse) and Figure 6 (longitudinal). As expected, the bias is significantly reduced using the more carefully selected set of records. A similar trend is evident when using the fundamental period in the longitudinal direction as the scale factor. Figure 7 shows the transverse response (the orthogonal component in this case) and Figure 8 shows the longitudinal response. Interestingly, the longitudinal PSDMs are un-conservatively biased; however, the plots are in linear space and are essentially equal. However, of greater interest in this study is whether using more than one period/intensity for scaling improves the agreement with the cloud analysis method. This comparison is made with the vector IM of IDA scaling strategy 5. The marginal PSDMs in the transverse and longitudinal directions are shown in Figure 9 and Figure 10, respectively. Unlike the transverse (IDA 1) and longitudinal (IDA 8) scaling strategies, the constant intensity stripes are evident in both the transverse and longitudinal directions. Regardless of what IDA record set was used, there is little to no bias in the median values. It should be noted that IDA 5 changes the original relative scaling between orthogonal components that is

maintained by other strategies.

A further means for comparing the different scaling strategies with the cloud results makes use of a vector of IMs when formulating the PSDM. The vector of IMs was not selected in order to reduce the dispersion of the demand model, rather to see whether the median response was biased based on different scaling strategies. An example of the vector PSDM (now resulting in a surface) generated for IDA 1 is shown in Figure 11. To avoid redundancy, a scaling-independent IM is used as the second IM in the vector. For the IDA 1 and 101 cases, the longitudinal IM $Sa(T_L)$ is normalized by $Sa(T_T)$, the IM used to scale the records. A best-fit plane was derived using least squares for each scaling method. The plane for the cloud method and the data points for IDA 1 and IDA 101 are shown in the figure. The best-fit (median square-root-sum-of-squares of the tangential drift ratio, Δ_{SRSS}) plane is described by four parameters, similar to those in Table 1. However, there is a coefficient for both $Sa(T_T)$ and $Sa(T_L)$. For the bridge considered in this study, larger demands were observed in the transverse direction and therefore, the magnitude of the $Sa(T_T)$ coefficient was larger than that of $Sa(T_L)$.

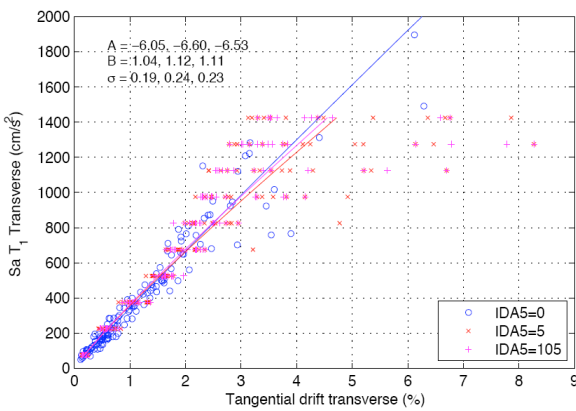


Figure 9. PSDM showing $Sa(T_T)$ - Δ marginal in the transverse direction for IDA scaling option 5.

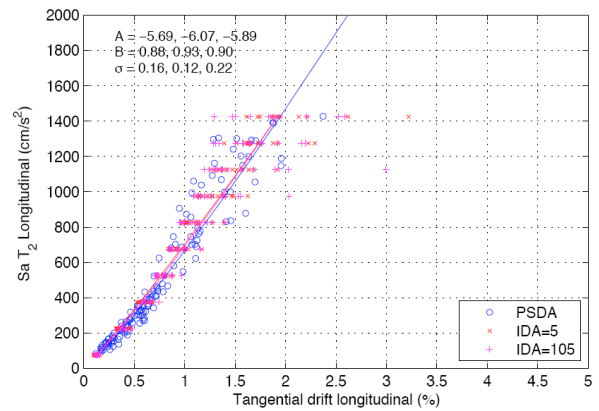


Figure 10. PSDM showing $Sa(T_L)$ - Δ marginal in the longitudinal direction for IDA scaling option 5.

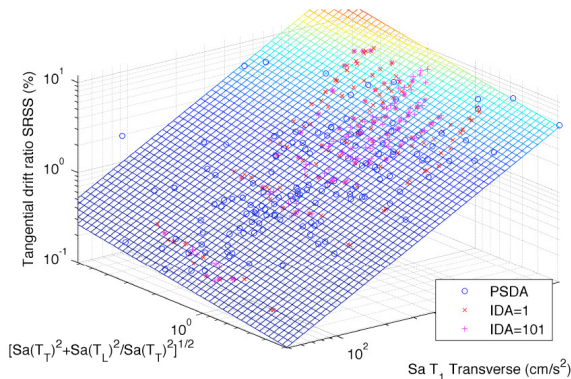


Figure 11. PSDM showing $Sa(T_T)$ transverse- and $Sa(T_L)$ longitudinal- Δ_{SRSS} for IDA scaling option 1.

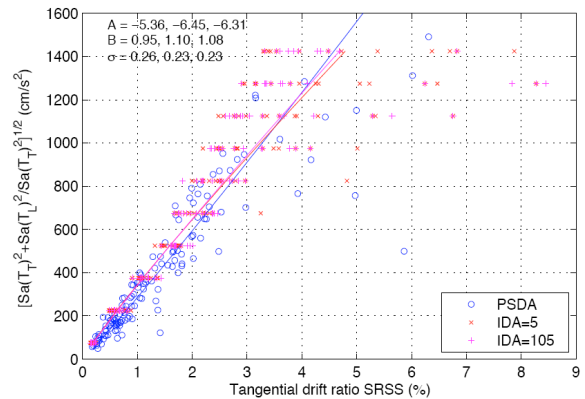


Figure 12. PSDM showing Δ_{SRSS} and SRSS of two IM quantities used in 3D PSDM.

Due to the difficulty of visualizing several planes for each scaling strategy, comparisons were drawn between scaling choices by calculating the residuals between the plane derived for each strategy and the plane derived from cloud analysis. Scaling strategies 3, 6, and 7 have the smallest residuals. Note, however, that it was not possible to evaluate strategy 5 in this manner because both IMs are dependent.

Therefore, a spectral combination was used to develop the Δ_{SRSS} PSDM with only a scalar IM, the SRSS of $Sa(T_T)$ and $Sa(T_L)/Sa(T_T)$. The resulting PSDMs for scaling strategy 5 are shown in Figure 12.

Conclusions

A typical reinforced concrete highway bridge is used in this study to investigate the effect of different ground motion scaling strategies on probabilistic seismic demand models for the global drift ratio response parameter. The bridge exhibits distinct transverse and longitudinal modes of response in the first two modes, respectively. Of the ten incremental dynamic analysis three-dimensional ground motion scaling techniques investigated in this paper, the optimal candidates were those that incorporate a spectral ordinate or spectral information from both the longitudinal and transverse directions (2, 3, 5, and 6). Results of scaling ground motions were compared to cloud demand analysis using a larger catalog of unscaled records. Random selection of records for IDA use leads to a bias in the marginal probabilistic seismic demand models in each direction. This is alleviated in part by selecting records based on the ratio of epsilon in the longitudinal direction to epsilon in the transverse direction. Values of this ratio close to positive one are optimal in reducing scaling irregularities between orthogonal ground motion components in three dimensions. However, the sign of each individual epsilon component should still be scrutinized to alleviate the bias due to the use of negative epsilon components. The choice of records with ϵ_L/ϵ_T in the vicinity of +1 is also beneficial in reducing the maximum scale factors required for achieving target intensity levels for all ground motion scaling strategies considered in this paper. A second option for scaling records that does not introduce bias for the structure considered in this study is the separate scaling of components in the transverse and longitudinal directions. This approach is akin to scaling records to a vector of intensities and results in greater control over the range of scale factors necessary in the non-scaling direction for other scaling strategies.

Acknowledgments

This work was supported in part by the Earthquake Engineering Research Centers Program of the National Science Foundation under award number EEC-9701568 through the Pacific Earthquake Engineering Research Center. Any opinions, findings, conclusions or recommendations expressed in this material are those of the author(s) and do not necessarily reflect those of the National Science Foundation.

References

- Abrahamson, N. A., and W. J. Silva, 1997. Empirical response spectral attenuation relations for shallow crustal earthquakes, *Seismological Research Letters* 68(1), 94-127.
- Baker, J. W., and C. A. Cornell, 2005. A vector-valued ground motion intensity measure consisting of spectral acceleration and epsilon, *Earthquake Engineering and Structural Dynamics* 34(10), 1193-1217.
- Brown, J., and S. K. Kunnath, 2004. Low-cycle fatigue failure of reinforcing steel bars, *ACI Materials Journal* 101(6), 457-466.
- Haselton, C. B., and J. W. Baker, 2006. Ground motion intensity measures for collapse capacity prediction: choice of optimal spectral period and effect of spectral shape, *Proceedings of the 8th US National Conference on Earthquake Engineering*, San Francisco, CA.
- Iervolino, I., and C. A. Cornell, 2005. Record selection for nonlinear seismic analysis of structures, *Earthquake Spectra* 21(3), 685-713.

- Kiremidjian, A., Moore, J., Fan Y. Y., Basoz, N., Yazali, O., and M. Williams, 2006. Highway demonstration project, *Report No. 2006/02*, Pacific Earthquake Engineering Research Center, University of California, Berkeley.
- Kunnath, S. K., and E. Kalkan, 2005. IDA capacity curves: The need for alternative intensity factors, *Proceedings of the 2005 ASCE Structures Congress*, New York, NY.
- Liao, K. W. and Y. K. Wen, 2004. Probabilistic demand and capacity analysis of 3-D steel frames under seismic excitations, *Proceedings of the 13th World Conference on Earthquake Engineering*, Vancouver, Canada.
- Liu, H., Goel, R., Bai, F., Scott, W., and T. Kono, 2006. Preliminary study on a 20-story office building instrumented by ANSS program in Anchorage, Alaska, *Proceedings of the 8th US National Conference on Earthquake Engineering*, San Francisco, CA.
- Mackie, K., and B. Stojadinovic, 2006. Seismic vulnerability of typical multiple-span California highway bridges, *Proceedings of the 5th National Seismic Conference on Bridges and Highways*, San Mateo, CA.
- Mackie, K. R., and B. Stojadinovic, 2005. Fragility basis for California highway overpass bridge seismic decision making, *Report No. 2005/02*, Pacific Earthquake Engineering Research Center, University of California, Berkeley.
- Shantz, T. J., 2006. Selection and scaling of earthquake records for nonlinear dynamic analysis of first mode dominant bridge structures, *Proceedings of the 8th US National Conference on Earthquake Engineering*, San Francisco, CA.
- Stewart, J. P., S-J. Chiou, J. D. Bray, R. W. Graves, P. G. Somerville, and N. A. Abrahamson, 2001. Ground motion evaluation procedures for performance-based design, *Report No. 2001/09*, Pacific Earthquake Engineering Research Center, University of California, Berkeley.
- Uriz, P., 2005. Towards earthquake resistant design of concentrically braced steel frames, *Ph.D. Thesis*, University of California, Berkeley.
- Vamvatsikos, D., 2006. Incremental dynamic analysis with two components of motion for a 3D steel structure, *Proceedings of the 8th US National Conference on Earthquake Engineering*, San Francisco, CA.
- Vamvatsikos, D., and C. A. Cornell, 2002. Incremental dynamic analysis, *Earthquake Engineering and Structural Dynamics* 31(3), 491-512.